

Wave-Mode Modification in Liquid Helium with Partially Clamped Normal Fluid*

GERALD L. POLLACK† AND J. R. PELLAM‡

California Institute of Technology, Pasadena, California

(Received 17 April 1964; revised manuscript received 15 October 1964)

When the equations of first and second sound are modified to correspond to wave propagation in the presence of viscous forces on the normal fluid, two wave modes result. In the limit of large viscous forces, second sound becomes an overdamped thermal mode with zero velocity, and first sound becomes an undamped (acoustic) mode with wave velocity v given to first order by $v^2 = (\rho_s/\rho)^2 c_1^2 + (\rho_n/\rho)^2 c_2^2$ in terms of usual symbols. In this investigation, the onset of wave-mode modification has been examined as degradation of pure second-sound pulses and standing waves in the presence of barriers. Normal fluid was partially clamped in the interstices of emery powder or rouge, with viscous drag controlled by employing several packing densities. The velocity of thermal signals sent through chambers filled with these small particles decreases, and the damping increases with smaller interstices. The theoretical wave velocities of the thermal and acoustic modes are obtained, as functions of temperature and a viscosity coefficient, from the modified wave equations. For suitably chosen constant values of the viscosity coefficient, the theoretical velocity of thermal waves is in approximate quantitative agreement with the observed pulse velocities, and the observations are interpreted in this way. Qualitatively observed attenuation is shown to be in agreement with the same theory. The effect of capacitive thermal losses to the barrier particles, and consequent possible degradation of incipient wave modes to thermal diffusion, is also analyzed.

INTRODUCTION

THE importance of wave phenomena in understanding the properties of liquid helium below the λ point (He II) has led to much fruitful study. So far, four kinds of waves have been predicted and identified: first sound,^{1,2} second sound,³⁻⁶ third sound,^{7,8} and fourth sound.^{9,10} First sound, acoustically excited pressure variation at constant entropy is, of course, a common physical phenomenon. Second sound, although so far only observed in liquid helium, is expected to exist in some dielectric solids.¹¹ Third and fourth sound are unique to liquid helium, as is a recently predicted¹² isobaric temperature wave.

The close connection between first and second sound in liquid helium has long been well appreciated. The two fluid hypothesis^{3,13,14} identifies those atoms in the ground state with a "superfluid"; all other atoms comprise a "normal" fluid. First sound, according to this

model, consists of pressure waves in which the two fluids move in phase. Second sound is the interflow of the two fluids out of phase with no net momentum transfer; it is a flow of entropy at constant density, and is observable as temperature waves. The transport of temperature differences according to a wave equation is very rare in nature; these experiments describe an investigation of a new wave of this kind excited thermally in liquid helium with partially or fully clamped normal fluid. The problem investigated is: What happens to the transmitted energy when a second sound wave impinges on a semi-impervious region? What kind of thermal wave or other thermal transport is allowed in the superfluid of helium II when the normal fluid is partially or fully clamped? Waves of this kind (fourth sound) were subsequently acoustically excited and observed by Rudnick and Shapiro.¹⁰

The interconvertibility of first and second sound was demonstrated¹⁵ in 1947 in the Yale effect experiments in which second sound was converted to first sound at a helium liquid-vapor interface. In addition, surprisingly, second sound produced in the liquid helium was picked up as pressure waves by an immersed microphone. At about this same time, Tisza¹⁶ showed the close theoretical interrelationship of these phenomena by deriving wave equations for both from a common Lagrangian. The two wave equations were shown to be satisfied by $\nabla \cdot \xi_1$ and $\nabla \cdot \xi_2$, sums and differences of the divergences of the vector fields formed by the displacements of normal fluid ξ_n and superfluid ξ_s multiplied by appropriate densities. Denoting normal fluid density, superfluid density, and total density, respectively, as ρ_n , ρ_s , and ρ then

$$\xi_1 = (\rho_n \xi_n + \rho_s \xi_s) / \rho, \quad (1a)$$

$$\xi_2 = (\xi_n - \xi_s) \rho_s / \rho. \quad (1b)$$

¹⁵ C. Lane, H. A. Fairbank, and W. M. Fairbank, *Phys. Rev.* **71**, 600 (1947).

¹⁶ L. Tisza, *Phys. Rev.* **72**, 838 (1947).

* This research has been supported in part by the Alfred P. Sloan Foundation, Inc.

† This article is based on a thesis submitted in partial fulfillment for the degree of Doctor of Philosophy from California Institute of Technology, 1962. Present address: National Bureau of Standards, Washington, D. C.

‡ Present address: The Garrett Corporation, Los Angeles, California.

¹ J. C. Findlay, A. Pitt, H. Grayson Smith, and J. O. Wilhelm, *Phys. Rev.* **54**, 506 (1938).

² J. R. Pellam and C. F. Squire, *Phys. Rev.* **72**, 1245 (1947).

³ L. Tisza, *J. Phys. Radium* **1**, 350 (1940).

⁴ L. D. Landau, *J. Phys. USSR* **5**, 71 (1941).

⁵ V. Peshkov, *J. Phys. USSR* **10**, 389 (1946).

⁶ J. R. Pellam, *Phys. Rev.* **75**, 1183 (1949).

⁷ K. R. Atkins, *Phys. Rev.* **113**, 962 (1959).

⁸ C. W. F. Everitt, K. R. Atkins, and A. Denenstein, *Phys. Rev. Letters* **8**, 161 (1962); *Phys. Rev.* **136**, A1494 (1964).

⁹ J. R. Pellam, *Phys. Rev.* **73**, 608 (1948).

¹⁰ I. Rudnick and K. A. Shapiro, *Phys. Rev. Letters* **9**, 191 (1962).

¹¹ M. Chester, *Phys. Rev.* **131**, 2013 (1963).

¹² K. A. Shapiro and I. Rudnick, *Bull. Am. Phys. Soc.* **8**, 613 (1963).

¹³ F. London, *Phys. Rev.* **54**, 947 (1938).

¹⁴ L. Tisza, *J. Phys. Radium* **1**, 164 (1940).

Using the equations of Tisza to explain the Yale effect, the conversion of second sound to first sound and the behavior of second sound at interfaces of all kinds was comprehensively analyzed in 1948.⁹ One result of the work was that if first or second sound were to impinge on a semi-impervious region, i.e., one in which there is a large viscous drag on the normal fluid only, two new kinds of wave modes would propagate through the superfluid. The equations of motion of the fluids under these conditions in terms of ξ_1 and ξ_2 are

$$\ddot{\xi}_1 + \frac{R}{\rho} \dot{\xi}_1 - c_1^2 \nabla^2 \xi_1 = -\frac{R}{\rho} \dot{\xi}_2, \quad (2a)$$

$$\ddot{\xi}_2 + \frac{\rho_s R}{\rho \rho_n} \dot{\xi}_2 - c_2^2 \nabla^2 \xi_2 = -\frac{\rho_s R}{\rho \rho_n} \dot{\xi}_1. \quad (2b)$$

The viscous force on unit volume of the normal fluid has been taken as $R\dot{\xi}_n$; c_1 and c_2 are the temperature dependent velocities of first and second sound. Assuming one-dimensional solutions of the form $\xi_1 = \xi_{10} e^{-\omega t} e^{i\alpha x}$ and $\xi_2 = \xi_{20} e^{-\omega t} e^{i\alpha x}$, the following results in the limit of large R , $R \gg \omega \rho_n$, are obtained.

The solution which may be identified as corresponding to second sound becomes a highly damped thermal wave for which

$$\left(\frac{\alpha}{\omega}\right)^2 = \frac{-iR(\rho_n c_2^2 + \rho_s c_1^2)}{\omega \rho \rho_n c_1^2 c_2^2} \frac{(\rho_n c_2^4 + \rho_s c_1^4)}{c_1^2 c_2^2 (\rho_n c_2^2 + \rho_s c_1^2)} + \dots \quad (3)$$

The solution corresponding to first sound is an undamped acoustic wave with velocity v :

$$v = \left(\frac{\rho_n c_2^2 + \rho_s c_1^2}{\rho} \right)^{1/2} \quad (4)$$

and attenuation α :

$$\alpha = + \frac{\omega^2 \rho_s \rho_n (c_2^2 - c_1^2)^2}{2R \rho v^3 c_2^2}. \quad (5)$$

The original analysis considered effects of viscosity only. In the present work, thermal absorption effects also will be examined. The wave of Eq. (4) has a velocity approaching c_1 near 0°K and approaching c_2 near the λ point. This wave would transmit through the viscous medium only that part of second sound which is converted to first sound at the semipermeable interface; the rest of the heat travels through the rouge in the highly overdamped mode.

Another way of posing this problem is by a consideration of the Fountain effect.¹⁷ Let a layer of rouge be packed into a tube which is immersed in liquid helium II so that the bath level is above the rouge but below the top of the tube. A light is then shone onto the upper rouge surface or heat is otherwise introduced to the

helium above the rouge. The result is that the helium in the tube rises. This means that in the limit of very low-frequency heating, thermal energy is somehow transmitted through the rouge. How is this energy transported?

The experiments to be described below have been thus aimed at investigating the two modes of heat transmission with emphasis on waves. For a semi-impervious region, varying grit sizes of emery powder were used as well as jeweler's rouge packed in densities increasing up to that attainable with a machine press. This variety provided some control over the magnitude of the viscous force on the normal fluid. To produce and detect the waves, three principle methods were employed: the pulse method,⁸ the standing-wave method,⁹ and, finally, an adaptation of the standing-wave method.

EXPERIMENT

I. The Pulse Method

On account of directness and ease of interpretation, it was decided to make the first attempt with the pulse method. Details of the method and a block diagram of the circuitry have been described previously.⁸ In all essentials, our apparatus and techniques are identical with those of the earlier work. The carbon-coated (800 Ω per square) Bakelite disks of 3–4 cm diameter used as thermal receiver and transmitter were separated by a Lucite annulus. Power output at the receiver was from 2–5 mW/cm². A cylindrical chamber of fixed height was thus provided through which the pulses were propagated. Measurements were made with various chamber heights, but since attenuation of the thermal pulses was later to become rather important, the receiver transmitter distance was fixed at 0.374 cm. Under these conditions, signals as small as 0.3 mdeg above the ambient helium could be observed. The small distance through which the waves traveled before impinging on the receiver made it possible to observe up to seven successive round-trip reflections of second sound in the chamber when it was filled with liquid helium II alone. Easy access of the helium to the chamber was provided by suitable holes in the receiver and transmitter. Using this technique $c_2(T)$ was measured between 1.25°K and the λ point, in excellent agreement with accepted values.

For measurement of the velocity of the pulses through helium with clamped normal fluid, the cylindrical space was filled successively with different grain sizes of emery powder or silicon carbide, with rouge at several packing densities, and, finally, with packed zeolite powder. The results for the velocity of the waves through emery powder of increasing fineness are presented on Figs. 1(a) through (g). The emery granules used were, respectively, (a) No. 46 grit size (sieve size 0.35 mm), (b) No. 100 grit (0.15 mm), (c) No. 150 grit (0.1 mm), (d) No. 200 grit (0.075 mm), (e) No. 320 grit (0.044 mm), (f) No. 400 grit (0.037 mm), and (g)

¹⁷ J. F. Allen and H. Jones, *Nature* **141**, 243 (1938).

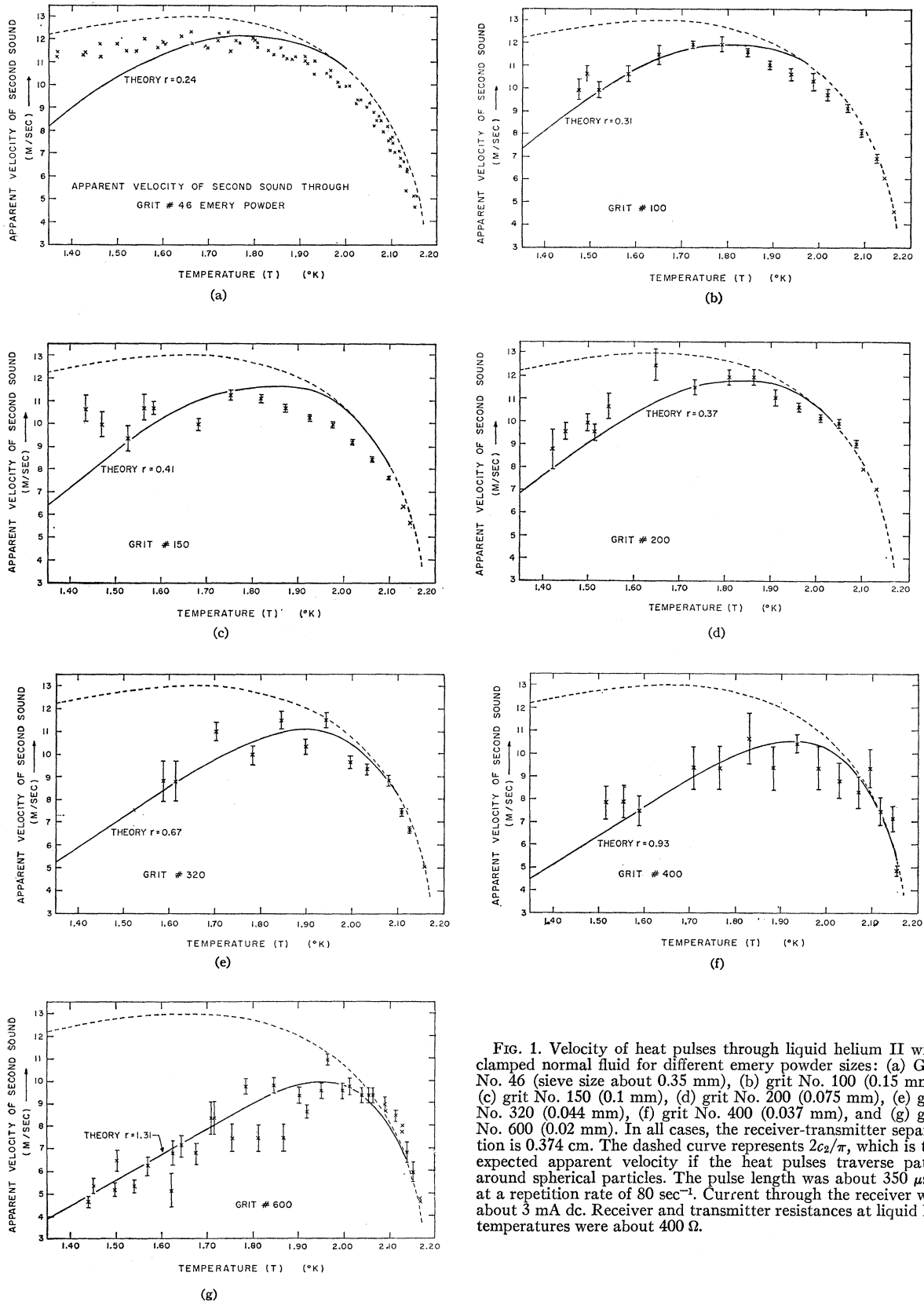


FIG. 1. Velocity of heat pulses through liquid helium II with clamped normal fluid for different emery powder sizes: (a) Grit No. 46 (sieve size about 0.35 mm), (b) grit No. 100 (0.15 mm), (c) grit No. 150 (0.1 mm), (d) grit No. 200 (0.075 mm), (e) grit No. 320 (0.044 mm), (f) grit No. 400 (0.037 mm), and (g) grit No. 600 (0.02 mm). In all cases, the receiver-transmitter separation is 0.374 cm. The dashed curve represents $2c_2/\pi$, which is the expected apparent velocity if the heat pulses traverse paths around spherical particles. The pulse length was about 350 μ sec at a repetition rate of 80 sec^{-1} . Current through the receiver was about 3 mA dc. Receiver and transmitter resistances at liquid He temperatures were about 400 Ω .

No. 600 grit (≈ 0.02 mm). Notice that the velocities of these waves are lower than that of second sound and much lower than that of the acoustic mode of Eq. (4). We shall show that these are explainable as thermal wave modes as in Eq. (3), but with intermediate values of R . The large errors indicated with the points on Fig. 1, especially at lower temperatures, are due to attenuation. Although the pulses were well defined at the transmitter, by the time they reached the receiver, even after only a single traversal, they were much smoothed out and otherwise attenuated. Only near the λ point and at the larger emery-particle sizes was it possible to observe multiple reflections. The velocity of the heat pulses decreases and the pulses suffer increasing attenuation as the temperature decreases and as the particle size decreases.

This effect was pursued further to finer particle sizes by substituting packed rouge for the emery powder. The results of this investigation for three different rouge densities are shown on Fig. 2. Rouge particles may be microscopically estimated as having diameters of about 10^{-3} mm. Notice that the velocity of the waves decreases as the rouge is packed more tightly (from 0.90 g/cm³ to 1.03 g/cm³), i.e., as the interstices get smaller. The attenuation also is observed to increase in this direction, and at rouge densities only 10% higher than 1.03 g/cm³, no received waves were observable over the background noise. The last attempt with this method was made using zeolite¹⁸ crystallites. Although the crystal structure contains very small channels of 10 Å diameter, the crystallites themselves are about 0.001 mm in diameter. Figure 3 is a plot of the apparent velocity of heat waves through helium trapped among zeolite crystallites which were packed tightly together with a machine press. From the similarity of the heat-pulse velocities in rouge and zeolite, it may be deduced that the effective channel size is the same, i.e., the heat pulses are probably being sent around the crystallites and not through the 10 Å channels as might be hoped.

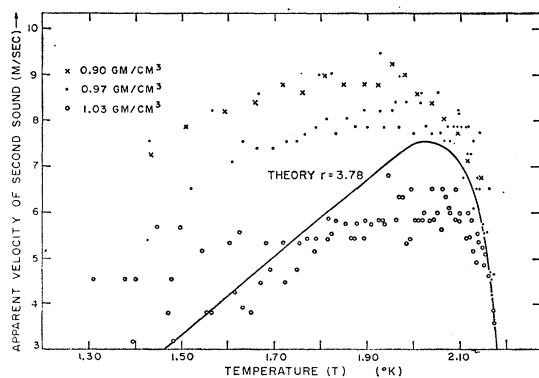


Fig. 2. Apparent velocity of second-sound pulses in liquid helium II as function of rouge density.

¹⁸ L. Broussard and D. P. Shoemaker, J. Am. Chem. Soc. 82, 1041 (1960).

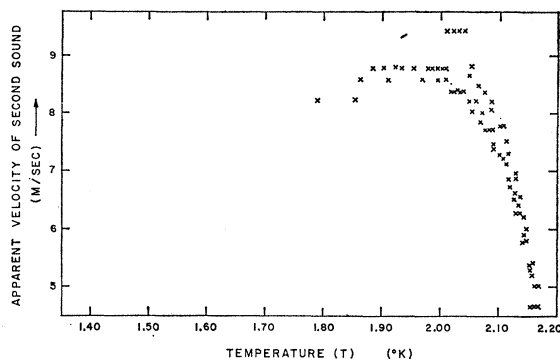


Fig. 3. Apparent velocity of second-sound pulses in liquid helium II with normal fluid clamped in zeolite.

If the particles are assumed to be spherical and the only physical effect of their interposition between the receiver and transmitter is to cause the second sound to pass around them through the liquid helium, then the apparent velocity of the heat pulses is expected to be $2c_2/\pi$. On Fig. 1, this curve is drawn in for each graph as a broken line. For this purpose, the $c_2(T)$ data measured with this same apparatus were used. Near the λ point, the above mechanism is adequate to describe what happens, since the measured points are rather close to the ideal curve. It may be seen, however, that as the temperature or the size of the interstices decreases, the experimental points diverge more and more from this dotted curve. The measurements in rouge and zeolite (Figs. 2 and 3) show a continuation of this trend.

There are two possible explanations for this degeneration of the second sound wave: frictional dissipation of energy due to slippage of the normal fluid, and thermal relaxation involving heat exchange with the barrier particles. The theory of each of these will be considered in the theoretical part of the paper. It will be shown there that the velocity decrease and attenuation are evidently due to the effects of incomplete normal fluid clamping. Thermal absorption gives effects in the right direction, but they are apparently too small to be observed.

The inherent disadvantage of the pulse method is that a wide-band amplifier must be used to receive the pulses. Since the minimal noise is proportional to the bandwidth in any amplifier, the attenuated waves were further pursued to greater rouge densities and consequent smaller channel sizes by a more sensitive technique—the standing-wave method.

II. The Standing-Wave Method

For these measurements, the classic techniques of Peshkov⁵ were only slightly modified. The receiver and transmitter were again, initially, carbon-coated disks separated by a fixed distance. Standing waves were excited in the helium with a signal generator connected to the transmitter element and a wave analyzer was used to measure the frequency and magnitude of tem-

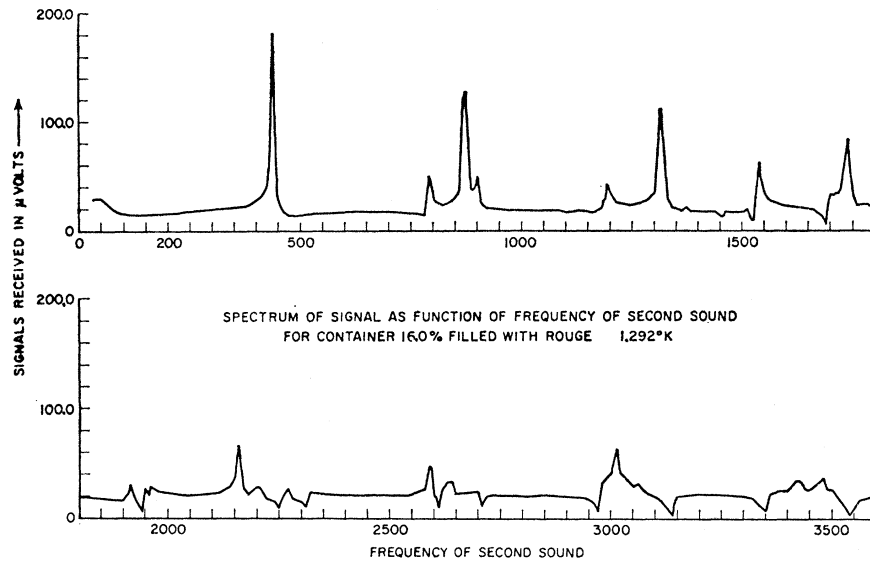


FIG. 4. Spectrum of signal as a function of frequency of second sound for container 16.0% filled with rouge, $T=1.292^{\circ}\text{K}$. The receiver and transmitter electrodes are concentric circles on a single disk placed at the mouth of the resonance cavity. At resonance, the temperature variation at the receiver reaches a maximum at twice the transmitted frequency and is observed with a wave analyzer. The well defined resonances shown indicate that most of the thermal energy is reflected from the rouge surface. Container depth before adding rouge was 2.69 cm.

perature fluctuations at the receiver, which carried a current of several milliamperes. The rouge was packed into the space between the receiver and transmitter to a density of 2.3 g/cm^3 in a machine press. When the rouge was omitted from the chamber, very well defined and large resonances were obtained, thus giving, as before, good measurements of second-sound velocity as a function of temperature. However, with the rouge in place, there were no observable resonances at all temperatures in the available range from 1.3°K to the λ point. Although this is an indication that the thermal energy is being absorbed, a more positive approach is preferred.

To this end, a flat-bottomed cylindrical cavity was bored in a solid block of Lucite. The receiver and transmitter were concentric annuli outlined with conducting concentric circles silver-painted on a single carbon-plated Bakelite disk. The disk fitted over the entrance to the cavity and ample holes were provided in it to permit free access of the helium to the chamber. The cavity was filled part way with rouge at the higher densities, and resonance spectra taken as follows: At each signal-generator frequency over a broad range ν , sent into the transmitter, the wave analyzer was tuned to 2ν , the frequency of the excited thermal waves, and the amplitude of the received signal was measured. In the next run, the rouge was removed and a Lucite wafer of the same thickness substituted for it. Since the rouge surface is a nodal surface for normal fluid velocity, but not superfluid velocity, and since the Lucite wafer surface is a nodal surface for both the normal fluid and superfluid velocity, any difference in the spectra for the two cases is due to superfluid which has penetrated the rouge surface.

Figure 4 shows a typical spectrum obtained in this manner with a rouge bottom to the free-resonance chamber. It is to be compared with a control spectrum

taken with a Lucite bottom to the chamber. The spectra were taken at the lowest temperatures attainable with the apparatus since the maxima were then more clearly defined and higher order harmonics were observable than at higher temperatures. In addition, at low temperatures the helium is almost entirely superfluid so it is expected that more of it can penetrate the barrier and flow in the rouge interstices bringing out data. To eliminate any possible effect of reflections from the closed bottom of the Lucite block under the rouge, spectra were taken with an open bottom, with identical results.

The most striking result of a comparison of the spectrum of Fig. 4 with its control is that they are qualitatively almost identical; barely a feature of each curve's profile is not repeated on the other. This means that all the fine structure is due, e.g., to coupling in cross modes of various orders, and to phase-sensitive interference between the background pickup and the second-sound resonances. There is one quantitative difference worth noting, however. The resonances from the resonance chamber with a Lucite bottom are significantly more slowly damped than the resonances from essentially the same chamber with a rouge bottom. In fact, even though the initial resonance from the Lucite ($150 \mu\text{V}$) was smaller than the initial resonance from the rouge ($180 \mu\text{V}$), the former spectrum clearly exhibits at least seven overtones, but the latter exhibits only six. This means that the rouge is not quite a hard surface to second-sound waves. Some of the thermal energy in the second sound is entering the rouge but not returning as waves. In some manner, this heat is degraded in the rouge channels. The waves which are reflected back from the rouge show exactly the resonance frequencies expected for a rigid bottom.

Figure 5 presents our most trenchant data on the mechanism of heat transmission through helium II

trapped in the rouge channels. To carry through this part of the experiment, the standing-wave technique was adapted, the previous apparatus being modified to provide continuously variable chamber heights. The disk containing the receiver and transmitter was attached to a rod running through seals in the dewar cap. The rod was suitably provided with a vernier scale so that the chamber heights could be measured to 0.001 in. Tuning by changing the distance of the receiver-transmitter from the rouge at a fixed frequency was much sharper than frequency tuning at fixed distance. On Fig. 5, each of the spectral scans is plotted with reference to the receiver-transmitter distance, from the upper rouge surface, shown by the vertical solid line next to it. The distance (chamber height) itself may be read from the abscissa scale. Spectra are all plotted with arbitrary but consistent units and the straight line corresponding to pure second sound reflected from the rouge surface as if it were impermeable, radiates out from the origin. The average temperature for these spectra is 1.296°K; near this temperature second-sound velocity changes only slowly with temperature. The line beginning at 8.5 on the ordinate axis and radiating upward corresponds to the signals that would be received from the bottom of the container, 5.16 cm below the surface of the rouge, if the waves of Eq. (4) were excited there.

It can be seen that much fine structure is associated with these spectra, and in order to determine what part of this is information coming from below the rouge surface, the experiment was repeated replacing the rouge surface by a wafer of Lucite. All of the scans in Fig. 5 and the control were extended well beyond the maximum ordinate displayed, but no signals from below the rouge were found. It may be shown that most of the peaks and troughs, except for the pure second-sound peaks, are due to excitation of crossmodes in the resonant chamber, enhanced by the axial symmetry of the receiver-transmitter element (concentric circle electrodes). Thus, again, the behavior of the rouge surface to thermal resonances matches the behavior of the Lucite surface in all essential details; all the peaks and valleys on the spectra of Fig. 5 are mirrored on control spectra. Consistent with our earlier findings that thermal energy is being degraded in the rouge, the reflections from the Lucite wafer are much stronger than from the rouge. The background level in this apparatus was low enough to permit detection by the wave analyzer of temperature fluctuations of only 2 μ deg. The deep troughs preceding some of the resonance peaks, especially at short chamber lengths, are due to interference between pickup and resonance signals. Sensitivity is not decreased on this account unless the resonance of the new waves is in a particularly unpropitious phase relation to the pickup. This difficulty was eliminated by taking data at more than one rouge thickness as well as several temperatures.

In these last experiments (Fig. 5), rouge occupies half the volume in which the new wave modes may be

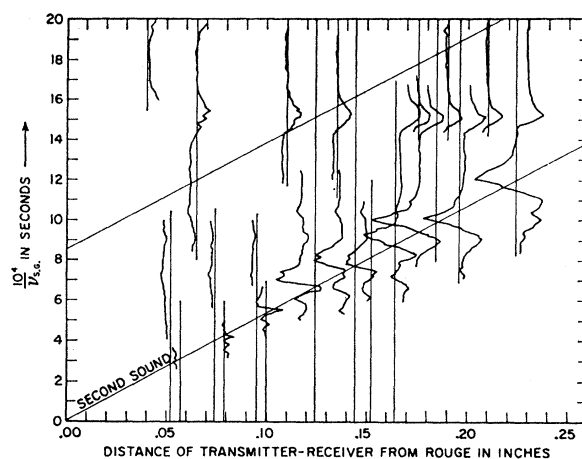


FIG. 5. Spectrum of signal height as a function of reciprocal of signal generator frequency, all measured at several chamber heights with rouge bottom. Each of the spectra was taken at the chamber height corresponding to the solid vertical line adjacent to it. At each of these heights, the wave analyzer at the receiver was continuously tuned to $2\nu_{s.g.}$ as the $\nu_{s.g.}$ was changed. When the second sound maxima from the rouge's upper surface are projected down to the vertical base lines, they lie close to the straight line emanating from the origin. The presence of the waves of Eq. (4) reflected from the bottom of the rouge would be indicated by similar maxima lying close to the straight line radiating up from 8.5 on the ordinate axis. Rouge was packed with a machine press to a depth of 5.16 cm. The average temperature was 1.296°K.

excited; the other half is occupied by clamped liquid helium II, and since the particles are small, there is ample surface for heat exchange and consequent degradation. The essence of the absorption might be then that temperature differences in rouge are brought to equilibrium by a diffusion equation and not a wave equation. The rouge in the bottom of the resonance chamber would be constantly conducting away the heat that is put in and in this way destroying the resonances. The best way to avoid this would be to find a substance which is as suitable as rouge in all ways but, for example, has a much lower thermal conductivity at these temperatures. Some of the standing wave experiments have been repeated with copper powder instead of rouge. The results were essentially unchanged.

Thus, it has not been possible to observe unattenuated waves by increasing the viscous force on the normal fluid. The essential question—how tightly clamped is the normal fluid in these experiments?—has interesting ramifications and deserves consideration.

For oscillatory flow of liquid helium II associated with a plane surface, the velocity in the fluid falls to e^{-1} of the velocity at the surface at distance $\delta = (2\eta_n/\omega\rho)^{1/2}$, in which η_n/ρ is the kinematic viscosity, and η_n is the viscosity of the normal fluid.¹⁹ Donnelly *et al.*²⁰ have measured η_n/ρ , obtaining at 1.1°K, 2×10^{-4} cm²/sec and at 2.1°K, 1.4×10^{-4} cm²/sec, with a smooth and slow

¹⁹ C. T. Lane, *Superfluid Physics* (McGraw-Hill Book Company, Inc., New York, 1962), pp. 47, 167.

²⁰ R. J. Donnelly, G. V. Chester, R. H. Walmsley, and C. T. Lane, *Phys. Rev.* **102**, 3 (1956).

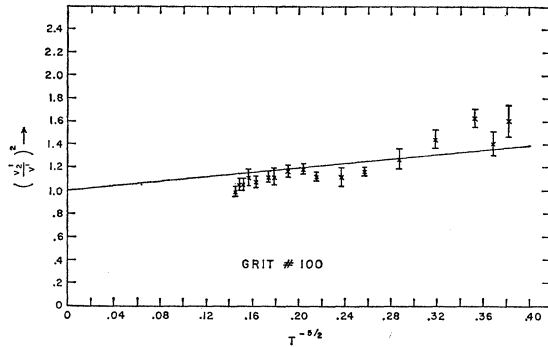


FIG. 6. Plot of $(v_2'/v')^2$ versus $T^{-5/2}$ for emery powder grit No. 100. Data is taken from Fig. 1(b). A straight line fitting all the points is consistent with a velocity decrease of the thermal waves due to heat absorption by the clamping medium.

variation at intermediate temperatures. The pulse train employed in our experiments consists of approximately trapezoidal pulses with repetition rate $(\omega_0/2\pi = T^{-1}) \approx 80 \text{ sec}^{-1}$, pulse length $(T_0) \approx 350 \mu\text{sec}$, and rise time (T_1) of the order of $1 \mu\text{sec}$. The Fourier cosine expansion of this pulse train has coefficients: $a_k = a_0(x^{-1} \sin x)(y^{-1} \sin y)$ with $x = k\pi T_1/T$ and $y = k\pi(T_0 + T_1)/T$. The characteristic frequency regions for the pulses are then: $(1/2T_0) \approx 1.4 \text{ kc/sec}$ and $(1/2T_1) \approx 500 \text{ kc/sec}$. The high-frequency coefficients are less important since they decrease as k^{-2} . This means that for effectively total clamping of normal fluid motion in both frequency modes, the pore size should be, respectively, 1.4×10^{-4} and 10^{-5} cm .

The actual pore sizes in the packed emery powder [see Fig. 1(a) through (g)] are not this small, strictly speaking, but instead are probably approximately equal to the respective sieve sizes, from 3.5×10^{-2} to $2 \times 10^{-3} \text{ cm}$. There is good reason to believe, however, that the effective pore size in the rouge experiments is small enough to clamp the normal fluid. A recent measurement²¹ of effective channel size in rouge packed with a ratio of (open volume)/(total volume) of 0.7 showed that the equivalent channel diameter for flow of liquid helium II was $1.8 \times 10^{-5} \text{ cm}$. In the experiments reported here, the ratio ranged from 0.8 in Fig. 2 to 0.5 in Figs. 4 and 5; the latter two are standing wave experiments. Earlier estimates²² of pore size in packed rouge are an order of magnitude lower than this.

Although δ is the distance between plane surfaces needed for effective clamping of normal fluid, where the channel geometry is irregular, as in the interstices of packed rouge and emery powder, actual pore sizes greater than δ may still clamp the normal fluid. We deduce therefore that in the rouge experiments the

²¹ J. B. Burnham, G. J. Pearson, J. Reppy, A. H. Speers, and C. A. Reynolds, in *Proceedings of the Seventh International Conference on Low Temperature Physics*, edited by G. M. Graham and A. C. Hollis Hallett (University of Toronto Press, Toronto, 1961).

²² J. F. Allen and A. D. Misener, *Proc. Roy. Soc. (London)* **A172**, 467 (1939).

normal fluid is effectively clamped and waves of pure superflow may, in this case, be precluded by the classical thermal diffusivity property of boundary materials. Since the experimental behavior of the velocity and attenuation of thermal pulses bends rather smoothly and monotonically through increasingly tightly packed emery powders to rouge, we might expect that thermal diffusion through emery particles is the principal determinant of the behavior of second sound pulses in those cases also. A theory of velocity decrease due to thermal diffusivity in the barrier materials is presented in the next section. The theory surprisingly fits the data better, the larger the interstices, and agrees only poorly with the data for liquid helium II in the interstices of tightly packed rouge; this is the reverse of expectations and an alternative, more satisfactory, theory is considered and shown to fit the experimental data.

THEORY

The lowering of wave velocity consequent upon passage through an absorbing medium is well known in acoustics and elsewhere. However, the effect is generally smaller and less dramatic than here. In analogy with the acoustical case, it may be shown that the lowering of the velocity of the heat waves through the emery powder below the value $2c_v/\pi$ is qualitatively, but not quantitatively, in accord with assuming heat absorption by the boundary material.

Where a temperature decrement ΔT exists in liquid helium, there arises a heat flux \dot{H} and these are related by

$$\dot{H} = (\rho c_v v_2') \Delta T, \quad (6)$$

where v_2' is the velocity of thermal waves in the medium and c_v is the specific heat of liquid helium. The thermal impedance of the liquid may then be expressed as $Z_{\text{th}} = 1/\rho c_v v_2'$. As in the case of electric waves on a transmission line, we define a thermal inductance L_{th} and a thermal capacitance C_{th} such that

$$Z_{\text{th}} = [L_{\text{th}}/C_{\text{th}}]^{1/2} \quad \text{and} \quad v_2' = [L_{\text{th}}C_{\text{th}}]^{-1/2}.$$

These lead us to the following equations for the thermal variables:

$$L_{\text{th}} = \frac{1}{\rho c_v v_2'^2} \quad \text{and} \quad C_{\text{th}} = \rho c_v. \quad (7)$$

The physical meaning of the thermal capacitance is clear. It is the amount of heat necessary to raise unit volume of the helium by one degree. Since in our case we have emery (or rouge) present in addition to the helium, we must add a term for it to the thermal capacity. This term will be temperature-dependent, and indeed it is expected to be proportional to T^3 . We assume then a new thermal capacity of the form

$$C_{\text{th}}' = \rho c_v + C_0 \quad (8)$$

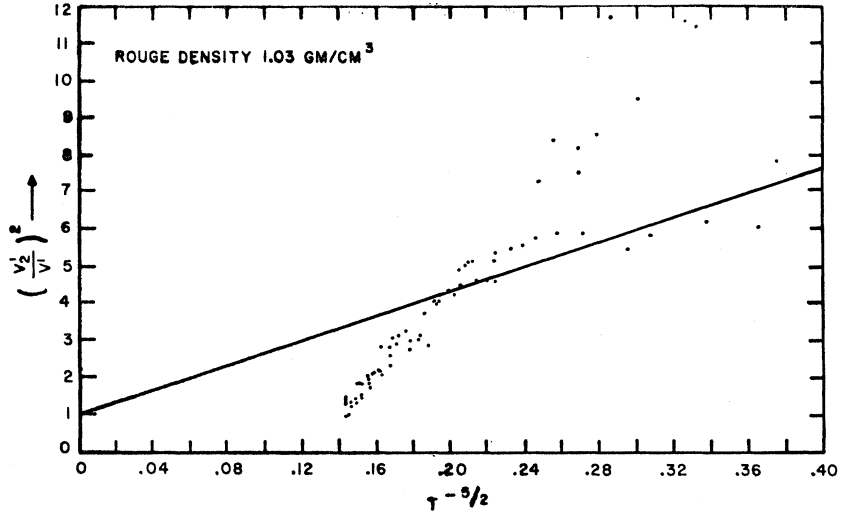


FIG. 7. Plot of $(v_2'/v')^2$ versus $T^{-5/2}$ for rouge of density 1.03 g/cm^3 . Data is taken from Fig. 2. The uncertainty in the data, as evidenced by scatter, is due to high attenuation of pulses, especially at low temperatures.

and the observed velocity (v') of thermal waves is then written

$$v' = \frac{1}{(L_{\text{th}} c_{\text{th}}')^{1/2}} = \frac{v_2'}{(1 + C_0/\rho c_0)^{1/2}}. \quad (9)$$

At the temperatures of the experiments, ρ is effectively constant and c_s is proportional to $T^{11/2}$, so Eq. (9) becomes

$$(v_2'/v')^2 = 1 + AT^{-5/2}, \quad (10)$$

where by v_2' is understood $2c_2/\pi$.

On Fig. 6 is plotted $(v_2'/v')^2$ versus $T^{-5/2}$ for a typical emery powder size. Notice that the fit of a straight line with intercept unity expected from Eq. (10) obtains rather well. This effect is probably spurious and the agreement of this theory with the data is not as satisfactory as expected. The tendency, discernible on Fig. 6, for high-temperature data to fall below the straight line and for low-temperature data to fall above it, increases as the particle size decreases. Figure 7 shows the extreme case of this in the plot of $(v_2'/v')^2$ versus $T^{-5/2}$ for the densest rouge packing through which pulses were received. There is another, perhaps more serious limitation. The straight lines on Figs. 6 and 7 have been given slopes optimal for fitting the data. The slope A in Eq. (10) can be estimated, only grossly, as 10^{-4} to 10^{-5} , i.e., the lines should be essentially horizontal.

The data support a natural and satisfactory explanation as incompletely clamped thermal wavemodes of the kind described by Eq. (3), but with small viscous coefficients.

If the indicated substitutions for ξ_1 and ξ_2 are made in Eqs. (2a) and (2b) and the determinant of the coefficients of the two resultant homogeneous simultaneous equations is equated to zero, an equation quadratic in (α^2) results. If now for convenience we set $\alpha = ik$ and introduce the dimensionless viscosity coefficient $r = R/\omega\rho$, the solutions to this equation may be

$$\left(\frac{\omega}{k}\right)^2 = \left\{ c_1^2 \left(1 + \frac{i\rho_s r}{\rho_n} \right) + c_2^2 (1 + ir) \pm \left[c_1^4 \left(1 - \frac{\rho_s^2 r^2}{\rho_n^2} + \frac{2i\rho_s r}{\rho_n} \right) + c_2^4 (1 - r^2 + 2ir) - 2c_1^2 c_2^2 \left(1 + \frac{\rho_s r}{\rho_n} + \frac{i\rho r}{\rho_n} \right)^2 \right]^{1/2} \right\} / 2 \left(1 + \frac{i\rho r}{\rho_n} \right). \quad (11)$$

In order to correctly identify the modes in the $r=0$ limit with their corresponding modes in the regions of intermediate and large r , the radical, which contains a complex quantity, must be simplified. Thus the exact solutions giving propagation constants for all r for both thermal and acoustic modes are reexpressed from Eq. (11) as

$$\left(\frac{\omega}{k}\right)^2 = \left\{ c_1^2 + c_2^2 \pm 2^{-1/2} [(a_1^2 + a_2 r^2 + a_3^2 r^4)^{1/2} + (a_1 - a_3 r^2)^{1/2}] \right\} \left\{ 2 \left(1 + \frac{\rho^2 r^2}{\rho_n^2} \right)^{-1} \left\{ 1 - \frac{i\rho r}{\rho_n} \right\} + \left\{ \frac{c_1^2 \rho_s r}{\rho_n} + c_2^2 r \pm 2^{-1/2} [(a_1^2 + a_2 r^2 + a_3^2 r^4)^{1/2} - (a_1 - a_3 r^2)^{1/2}] \right\} \right\} \left\{ 2 \left(1 + \frac{\rho^2 r^2}{\rho_n^2} \right)^{-1} \left\{ i + \frac{\rho r}{\rho_n} \right\} \right\} \quad (12)$$

in which

$$a_1 = (c_1^2 - c_2^2)^2, \quad (12a)$$

$$a_2 = 2[2(c_1^4 \rho_s / \rho_n + c_2^4 - c_1^2 c_2^2 \rho / \rho_n)^2 - a_1 a_3], \quad (12b)$$

and

$$a_3 = (\rho_s c_1^2 / \rho_n + c_2^2)^2. \quad (12c)$$

This form of the expansion holds when the imaginary part of the quantity in the radical of Eq. (11) is greater than zero, i.e.,

$$2r(c_1^4\rho_s/\rho_n+c_2^4-c_1^2c_2^2\rho/\rho_n)>0. \quad (13)$$

Equation (13) is satisfied from just below the λ point throughout the range of observation.

In the limit $r=0$, the thermal mode may be identified in Eq. (12) as that for which $(\omega/k)^2=c_2^2$ by choosing the *minus* sign of the \pm sign in front of the two radicals, which now contain real, positive quantities. The acoustic mode corresponds to the solution with the *plus* sign in front of the radicals, and gives $(\omega/k)^2=c_1^2$ in the $r=0$ limit. In this notation, for complex k , the wave velocity is given by $\omega/\text{Re}(k)$, and the attenuation by $\text{Im}(k)$.

A good approximate formula for the velocity of thermal wave modes, suitable for comparison with the data, may be derived from Eq. (11). Since over the range of observation, $c_2^2 \ll c_1^2$, the radical in Eq. (11) may be approximated by entirely neglecting all terms in c_2^4 , keeping one small term in (c_2^2/c_1^2) in a binomial expansion of the radical and noticing that

$$(1-\rho_s^2r^2/\rho_n^2+2i\rho_s r/\rho_n)^{1/2}=1+i\rho_s r/\rho_n.$$

The result is

$$\left(\frac{\omega}{k}\right)^2 = \frac{c_2^2}{1+i\rho_s r/\rho_n} \quad (14)$$

from which the velocity (v_{th}) and the attenuation of the

thermal wave mode are

$$v_{\text{th}} = \sqrt{2}c_2 / [(1+\rho_s^2r^2/\rho_n^2)^{1/2}+1]^{1/2}, \quad (15a)$$

$$\text{attenuation} = (\omega/\sqrt{2}c_2) [(1+\rho_s^2r^2/\rho_n^2)^{1/2}-1]^{1/2}. \quad (15b)$$

The parameter r has been chosen to match the data in Figs. 1 and 2 at 1.7°K. Calculated v_{th} from Eq. (15a) as functions of temperature are shown on Figs. 1(a) through 1(g) and in Fig. 2. The corresponding results are: grit No. 46 emery, $r=0.24$; grit No. 100, $r=0.31$; grit No. 150, $r=0.41$; grit No. 200, $r=0.37$; grit No. 320, $r=0.67$; grit No. 400, $r=0.93$; grit No. 600, $r=1.31$; and rouge of 1.03 g/cm³, $r=3.78$. For convenient comparison with experiment, the graphed velocities have all been multiplied by $(2/\pi)$. This means that the waves are still assumed to be going around barrier particles which are approximately spherical. The theoretical fit to the data is generally quantitatively satisfactory. In addition, there is no strong reason why r could not be temperature-dependent. A temperature-dependent r could significantly improve the fit.

The theoretical attenuation of thermal modes, as given in Eq. (15b) increases with decreasing temperature (through ρ_s/ρ_n), and with decreasing channel diameter (through r). These are in agreement with the observed qualitative behavior of the pulse attenuation. Further affirmation requires quantitative attenuation measurements.

We conclude from these arguments that the observed pulse wave modes are principally due to the modified thermal waves associated with incompletely clamped normal fluid.